STUDY OF ZnO and V_2O_5 NANOPARTICLES AS HETEROGENEOUS PHOTOCATALYSTS IN DEGRADING ORGANIC POLLUTANTS

Yim Leng Chan, Swee Yong Pung, and Srimala Sreekantan

School of Materials and Mineral Resources Engineering, Engineering Campus,
Universiti Sains Malaysia, Pulau Pinang, Malaysia
Tel: 60-6045995215, e-mail: sypung@usm.my

Received Date: September 24, 2013

Abstract

Heterogeneous photocatalysis particularly using semiconductor material to degrade organic compound is intensively studied in recent years. Semiconductors are good photocatalysts attributed to theirs light absorption properties, carrier charge transport characteristics and excited-state lifetimes. In this work, mixture of ZnO (3.23 eV) and V_2O_5 (2.38 eV) nanoparticles were used to degrade RhB solution under UV and visible light irradiation, respectively. The rod-like ZnO nanoparticles have an average diameter of 244.1 ± 94.5 nm whereas spherical-like V_2O_5 nanoparticles have an average diameter of 231.9 ±14.0 nm. Under UV light irradiation, pure ZnO nanoparticles have the highest photodegradation efficiency with rate constant of 0.034 ± 0.004 min^{-1}. This was attributed to its high reducing power of electrons and oxidation power of holes for producing free radicals. On the contrary, pure V_2O_5 nanoparticles demonstrated the highest photodegradation efficiency with rate constant of 0.013± 0.001 min^{-1} under visible light irradiation since it has profusion absorption in visible light region. The result provides useful guideline for designing a waste water purifier driven by sunlight for organic pollutants removal based on a mixture of wide bandgap and narrow bandgap semiconductor nanomaterials.

Keywords: Organic dyes, Photocatalysis, Semiconductor, ZnO, V_2O_5

Introduction

Pollutant particularly from textile and agriculture industries is produced at the rate of approximately 2 million tons per year and is discharged into water system. This issue has become health concern throughout the globe. Various approaches have been used to treat the organic pollutants in order to minimize the rate of water pollution. However, these approaches which include Fenton [1], precipitation [2] and reverse osmosis [3] cause secondary pollution to the environment. Advanced oxidation process (AOP) [4] is one of the water treatments used to degrade organic pollutants from polluted water system. It utilizes mainly semiconductor photocatalysts in the degradation process. It involves electrical and chemical reaction on the semiconductor photocatalyst surface in the presence of light. Electron-hole pairs are generated when the absorption energy of photon (light) is greater than the energy bandgap of semiconductor photocatalysts. These charge carriers are needed to produce free radicals for degradation of organic compounds [5]. In addition, AOP is capable of minimizing the organic pollution at low cost. It degrades the organic compounds into harmless by-product such as water, carbon dioxide and mineral acids. Thus, this approach does not produce secondary pollutants [6].

Wide bandgap semiconductors such as titanium oxide (TiO_2) [7], cadmium sulfide (CdS) [8], iron oxide (Fe_2O_3) [9] and zinc oxide (ZnO) [10] are commonly used in AOP. These photocatalysts are sensitive to UV light (wavelength from 200 nm to 400 nm). The photogenerated charge carriers from these wide bandgap semiconductors under UV irradiation have a higher free energy that is required for producing free radicals. However, low bandgap semiconductors such as V_2O_5 and MnO_2 are more adapted to the solar spectrum as solar spectrum composes of 44 % of visible light and < 3 % of UV light. Thus, the photodegradation efficiency of using semiconductor photocatalysts can be further improved by developing the visible light driven photocatalysts. Many researches have been done recently for the development of more efficient photocatalysts that response to the visible light irradiation. For examples, Yousef *et al.* reported that the photocatalytic activity in visible light was increased using Cd-doped ZnO synthesized by electro-spinning [11]; Wang *et al.* achieved a better photodegradation efficiency using ZnO-CdS core-shell nanocomposites produced by hydrothermal [12].

In this work, the photodegradation efficiency on organic pollutant by a mixture of semiconductor photocatalysts under ultraviolet and visible light was studied, respectively. The optimum ratio of semiconductor photocatalysts to degrade Rhodamine B (RhB) solution determined from this study provides useful information for the subsequent work to set up a waste water purifier that based on semiconductor nanomaterials that grown on flexible polymer fibers. Zinc oxide was chosen because of its wide bandgap (3.37 eV), large binding energy (60 meV), long term stability and non-toxic in nature. The crystal structure of ZnO could be described as a number of alternating planes composed of tetrahedral coordinated O^{2-} and Zn^{2+} stacked along the *c*-axis [13]. ZnO can be used for a number of applications such as NO_2 gas sensor, UV laser [14], light emitting diode [15], solar cell [16] and piezoelectric nanogenerator [17]. On the other hand, vanadium oxide (V_2O_5) was chosen because of its narrow bandgap (2.80 eV). It has variety of vanadium oxidation states, ranging from 2^+ to 5^+ and variability of oxygen coordination geometry. The structure of V_2O_5 is zigzag ribbons which compose of square pyramid VO_5 units. These VO_5 units share their edges and thus build double chains along the b direction [18]. The common applications of V_2O_5 are optical switching device [19] and solar cell [20]. The RhB solution was chosen as organic pollutant because it is one of the most widely used Xanthene dyes in textile industry and becomes a common organic pollutant in water system. Xanthene dyes are organic heterocyclic compounds that can be prepared by condensation of derivates of phthalic anhydride with derivates of resorcinol.

Methodology

Analytical grade of V_2O_5 powder was purchased from Sigma Aldrich Company and ZnO powder was purchased from Merck Company. The morphologies of the nanoparticles were examined by Zeiss Supra 35 VP field emission scanning electron microscope (FESEM). The phase and crystallinity of the nanoparticles were characterized using a Philip PW 1729 X-ray diffractometer (Cu K_α, $\lambda = 0.154$ nm). The bandgap of nanoparticles was determined from Perkin UV-Vis spectrometer.

Photocatalytic activities of semiconductor nanoparticles were evaluated by degradation of RhB solution (1×10^{-5} M) under the illumination of light at room temperature. The mixture of V_2O_5 and ZnO nanoparticles in certain ratios were prepared in 20 ml of RhB solution. The ratios of ZnO and V_2O_5 were 1:0, 0.75:0.25, 0.5:0.5, 0.25:0.75 and 0:1. These solutions were irradiated by visible light using Philips bright boost super 80 tube lamp (555 nm) and were irradiated by UV light using Philip TUV 18W 1SL lamp (254 nm), respectively. The solution was sampled periodically from the quartz tube to monitor the degradation of RhB. The deterioration of RhB as a function of irradiation time was determined using Cary 50 spectrometer.

Results and Discussion

V_2O_5 Nanoparticles

The crystal phase of the semiconductor nanoparticles was analysed by X-ray diffraction (XRD). The XRD pattern of nanoparticles could be indexed as V_2O_5 (refers to JCPDS 60-767) as shown in Figure 1(a). No diffraction peaks for other polymorphous V_2O_5 was detected. The morphology of the V_2O_5 nanoparticles obtained was sphere-like nanostructures as indicated in Figure 1(b). The V_2O_5 nanoparticles have an average diameter of 231.9 ± 14.0 nm. The bandgap (E_g) of V_2O_5 nanoparticles was 2.38 eV as measured by Perkin UV-Vis spectrometer. The conduction band edge (E_c) and valence band edge of V_2O_5 with respect to vacuum as the zero energy reference of calculated from equations (1) and (2) (where X is the electronegativity), are -4.91 eV and -7.29 eV, respectively [21].

$$E_c = -X + 0.5E_g \tag{1}$$
$$E_V = -X - 0.5E_g \tag{2}$$

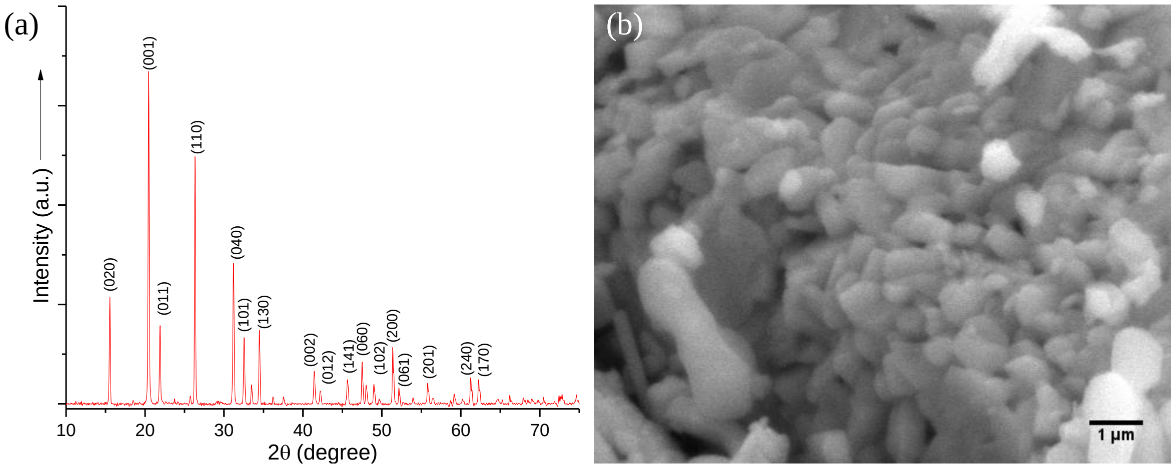

Figure 1. (a) XRD pattern and (b) SEM image of V_2O_5 nanoparticles

ZnO Nanoparticles

XRD analysis of the nanoparticles could be indexed to hexagonal ZnO (JSPDS Card No. 41-488) as shown in Figure 2(a). The diffraction peaks at 31.77 °, 34.42 °, 36.25 °, 47.54 °, 56.60 °, 62.86 °, 66.38 °, 67.96 °, and 69.10 ° are corresponded to (100), (002), (101), (102), (110), (103), (200), (112) and (201) crystal planes respectively. The FESEM images show that the rod-like nanostructures have an average diameter of 244.1 ± 94.5 nm as shown in Figure 2(b). Thus, ZnO nanoparticles and V_2O_5 nanoparticles used in the subsequent photocatalytic study was closed to each other, minimizing the effect contributed by the size of the particles. The bandgap of ZnO determined by Perkin UV-Vis spectrometer is 3.23 eV with -4.17 eV conduction band edge and -7.40 eV valence band edge respect to vacuum as zero energy reference.

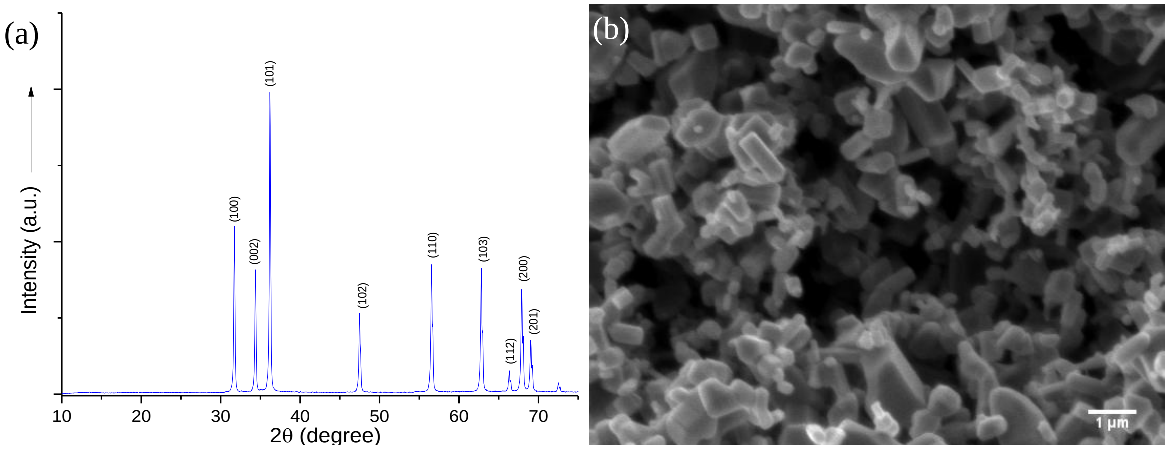

Figure 2. (a) XRD pattern and (b) SEM image of ZnO nanoparticles

Degradation of RhB Solution under UV Light

The effectiveness of semiconductor nanoparticles with different ratio of V_2O_5 and ZnO nanoparticles to degrade RhB solution under UV light (254 nm) was evaluated. The degraded RhB solution by these semiconductor nanoparticles was characterized by measuring the 553 nm absorption spectra of RhB using UV-Vis spectroscope. Under UV-light irradiation, but in the absence of ZnO nanoparticles, the absorbance of RhB changed little after irradiation (Figure 3). This indicates that the photo-induced self-sensitized photolysis of RhB can be neglected. However, the photodegradation was enhanced when ZnO nanoparticles were added as catalysts. The RhB solutions turned into lighter colour with a longer irradiation time. Figure 4(a) shows the UV-Vis absorption spectrum of RhB solution using 0:1 of ratio ZnO and V_2O_5 nanoparticles as a photocatalyst. The intensity of the 553 nm absorption peak decreased as a function of irradiation time. The decrease of this absorption peak was due to the breaking of the conjugated π-system in RhB chain. The intensity of RhB decreased from 1.293 a.u. (0 min) to 0.895 a.u. after 30 min irradiation. It further reduced to 0.838 a.u. after 60 min, 0.760 a.u. after 90 min and 0.608 a.u. after 120 min irradiation. Similar observation i.e. deterioration of RhB solution over irradiation time applied to other ratios of ZnO and V_2O_5 nanoparticles.

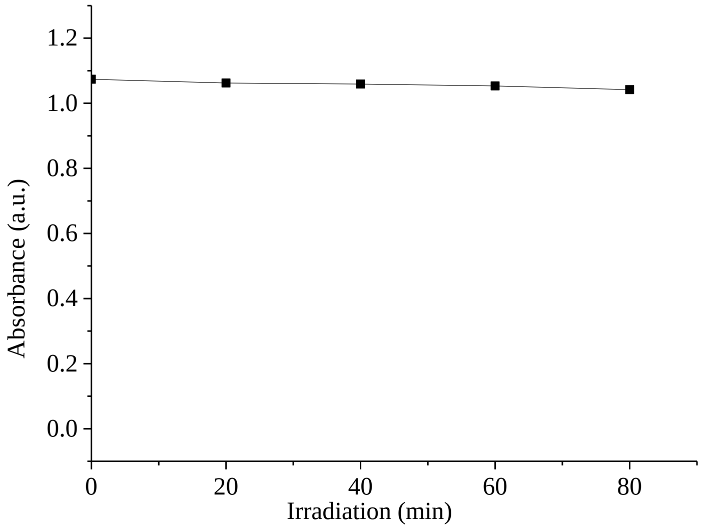

Figure 3. Degradation of RhB solution under UV light irradiation without using ZnO nanoparticles

The concentration of the RhB solution is proportional to the absorption as stated in Beer-Lambert law. Figure 4(b) shows the normalized absorbance of RhB solution degraded by 0:1 ratio of ZnO and V_2O_5 nanoparticles versus UV irradiation exposure time. Generally, the linear plots of $\ln(C_o/C)$ versus irradiation time indicates that the degradation of RhB solution followed first order kinetic (where C_o = initial concentration of RhB and C = concentration of RhB after irradiation). The rate constant of 0:1 ratio of ZnO and V_2O_5 nanoparticles is 0.0065 ± 0.0006 min^{-1} as determined from the slope of the graph.

The rate constant for different ratio of photocatalysts for degrading RhB solution under UV irradiation exposure time is shown in Figure 5. The rate constant decreased with decreasing of ZnO nanoparticles from 0.0340 ± 0.0039 min^{-1} (1:0 ratio) to 0.0065 ± 0.0006 min^{-1} (0:1 ratio). Pure ZnO nanoparticles have the highest photodegradation efficiency than pure V_2O_5 nanoparticles under UV irradiation. This result could be attributed to the decomposition of RhB involves photo-excitation of semiconductor photocatalysts. The excited electrons in conduction band need to be able to reduce the oxygen molecules into oxygen free radicals whereas the holes in the valence band need to be able to produce hydroxyl free radicals. The photodegradation efficiency of RhB solution is greatly dependent on the number of these free radicals.

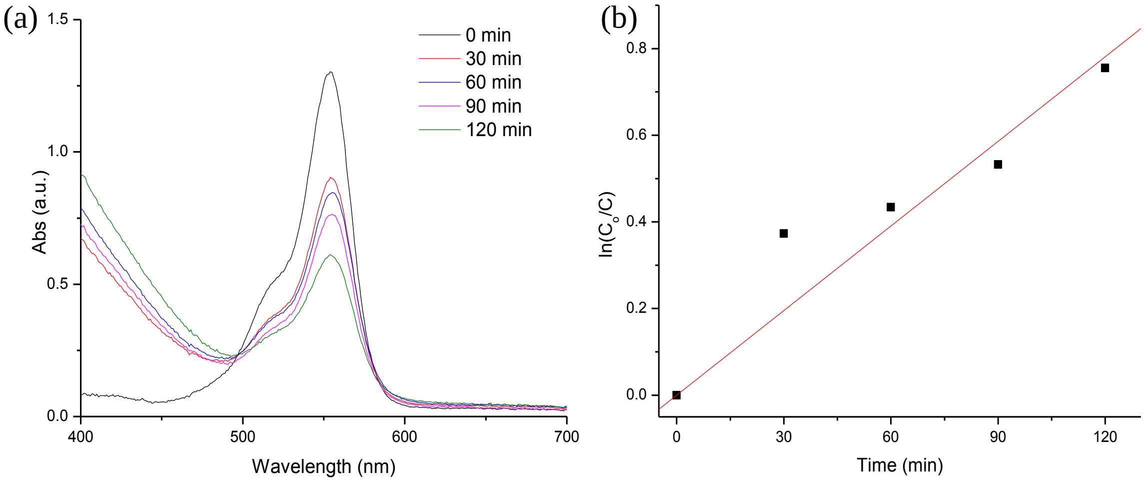

Figure 4. (a) Temporal change in concentration of RhB monitored at 553 nm and (b) normalized absorbance of RhB at 553 nm versus UV irradiation exposure time for 0:1 ratio of ZnO and V_2O_5 nanoparticles under UV light irradiation

In the case of ZnO nanoparticles, the electrons in the conduction band are high in reducing power and holes in the valence band are high in oxidizing power [21]. The conduction band edge of ZnO, i.e. -0.20 eV is more negative to the absolute electronegativity of oxygen (-0.046eV). Thus, the excited electrons are able to reduce the oxygen molecules into free radicals. On the contrary, the valence band edge of ZnO, i.e. 3.17 eV is more positive than the oxidation potential of water (redox potential of O_2/H_2O couple - 1.99 eV) and able to produce free radicals. The photodegradation efficiency under UV irradiation was reduced significantly with reducing amount of ZnO nanoparticles in the mixture as shown in Figure 5. On the contrary, V_2O_5 nanoparticles showed negligible photocatalytic activity in this study. This could be attributed to its lack of absorption in the UV region [22].

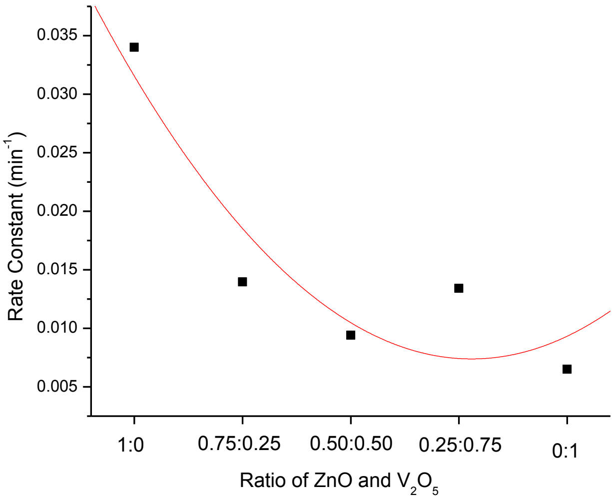

Figure 5. Photodegradation of RhB solution by different ratio of ZnO:V_2O_5 nanoparticles under UV irradiation

Degradation of RhB Solution under Visible Light

The photocatalytic activity of ZnO and V_2O_5 to degrade RhB under visible light was studied. The absorption spectra of RhB solution using 0:1 ratio of ZnO and V_2O_5 nanoparticles under visible light is shown in Figure 6(a). The absorption peak at 553 nm decreased from 1.293 a.u. (intial absorption) to 0.519 a.u. after 60 min visible light irradiation. The linear line of In(Co/C) versus irradiation time in Figure 6(b) indicates that the photodegradation of RhB solution followed the first order kinetic. The rate constant determined from the slope of this graph is 0.0130 ± 0.0012 min^{-1}.

The rate constant as a function of ratio of ZnO and V_2O_5 nanoparticles under visible light is plotted in Figure 7. A minimum curve was obtained. The RhB solution was degraded under visible light irradiation at 100 % of ZnO nanoparticles with rate constant of 0.0108 ± 0.0008 min^{-1}. This observation is unexpected as ZnO should not response to visible light attributed to its wide energy bandgap (3.23 eV). The presence of defects such as oxygen vacancies in the ZnO nanoparticles, which induced energy levels in its bandgap, could be responsible to the generation of electrons and holes for producing free radicals that degraded the RhB solution [23]. The rate constant was reduced with ZnO nanoparticles and achieved the minimum value of 0.0026 ± 0.0003 min^{-1} at the ratio of 0.50:0.50 of ZnO and V_2O_5 nanoparticles. The contribution of V_2O_5 nanoparticles to degrade RhB solution was dominant after 0.50:0.50 ratio. The V_2O_5 nanoparticles absorbed the visible light effectively to produce free radicals for degradation of RhB solution attributed to its narrow bandgap. It achieved the highest photocatalytic efficiency with rate constant of 0.0130 ± 0.0012 min$^{-1.}$

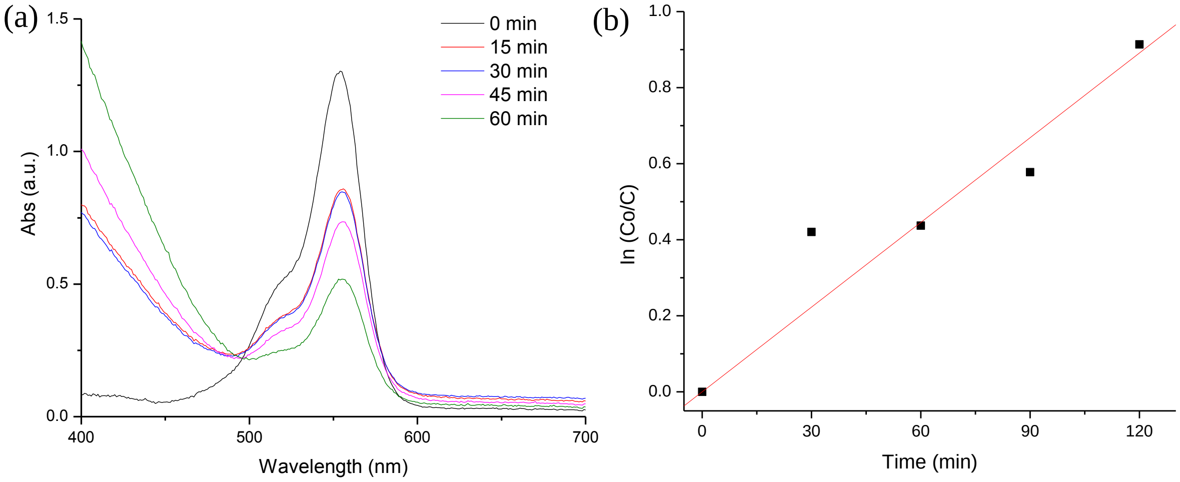

Figure 6. (a) Temporal change in concentration of RhB monitored at 553 nm and (b) normalized absorbance of RhB at 553 nm versus UV irradiation exposure time for 0:1 ratio of ZnO and V_2O_5 nanoparticles under visible light

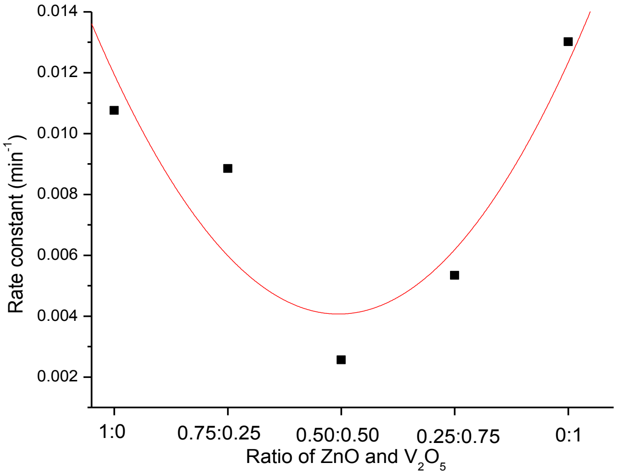

Figure 7. Photodegradation of RhB solution by different ratio of ZnO:V_2O_5 nanoparticles under visible light irradiation

Conclusions

The photodegradation efficiency of mixture of ZnO and V_2O_5 nanoparticles with different bandgap to degrade RhB solution under UV and visible light irradiation was studied. The ZnO nanoparticles used in this work have a rod-like structure with an average diameter of 244.1 ± 94.5 nm whereas V_2O_5 nanoparticles have a spherical-like structure with average diameter of 231.9 ±14.0 nm. The bandgap of ZnO nanoparticles and V_2O_5 nanoparticles measured via UV-Vis spectrometer was 3.23 eV and 2.38 eV, respectively. The study showed that pure ZnO nanoparticles have the highest photodegradation efficiency with rate constant of 0.034 ± 0.0039 min^{-1} under UV light irradiation. This was attributed to its high reducing power and oxidation power for producing free radicals. On the contrary, V_2O_5 nanoparticles demonstrated the highest photodegradation efficiency with rate constant of 0.013 ± 0.0012 min^{-1} under visible light irradiation since it has profusion absorption in visible light region. This result provides preliminary guideline for subsequent study on the photodegradation of RhB solution using mixture of ZnO and V_2O_5 nanoparticles under sunlight which composes of 44 % of visible light and < 3 % of UV light.

Acknowledgement

The authors would like to acknowledge Universiti Sains Malaysia (Research University grant, 1001/PBAHAN/814200) for the financial support to conduct this project.

References

[1] X. Fan, H. Hao, X. Shen, F. Chen, and J. Zhang, "Removal and degradation pathway study of sulfasalazine with fenton-like reaction," *Journal of Hazardous Materials*, Vol. 190, No. 1-3, pp. 493-500, 2011.

[2] N. Riaz, N. Ela, M.S. Khan, F.K. Chong, and B.K. Dutta, "Effect of photocatalysts preparation methods and light source on orange II photocatalytic degradation," *Environmental Science and Technology*, Vol. 6, pp. V2-112 to V112-117, 2011.

[3] C. Baudequin, E. Couallier, M. Rakib, I. Deguerry, R. Severac, and M. Pabon, "Purification of firefighting water containing a fluorinated surfactant by reverse osmosis coupled to electrocoagulation-filtration," *Separation and Purification Technology*, Vol. 76, No. 3, pp. 275-282, 2011.

[4] J. Fu, Y. Tian, B. Chang, F. Xi, and X. Dong, "BiOBr-carbon nitride heterojunctions: Synthesis, enhanced activity and photocatalytic mechanism," *Journal of Materials Chemistry*, Vol. 22, No. 39, pp. 21159-21166, 2012.

[5] G. Pyrgiotakis, and W. Sigmund, "Photocatalytic particles for biocidal applications," In *Particulate System in Nano- and Biotechnologies*, H. Ei-Shall, D.O. Shah, W. Sigmund, and B.M. Moudgil, eds.: Taylor & Francis Group, Boca Raton, Florida, United States, pp. 283-307, 2009.

[6] P. Pichat, "Photocatalytic degradation of pollutants in water and air: Basic concepts and application," In *Chemical Degradation Methods for Wastes and Pollutants*, M.A. Tarr, ed.: CRC Press, Boca Ranton, Florida, United States, 2003.

[7] J. Zhuang, W. Dai, Q. Tian, Z. Li, L. Xie, J. Wang, *and P. Liu*, "Photocatalytic degradation of RhB over TiO_2 bilayer films: effect of defects and their location," *Langmuir Article*, Vol. 26, No. 12, pp. 9686-9694, 2010.

[8] C. Liu, Z. Liu, Y. Li, Z. Liu, Y. Wang, L. E*, J. Ya, N. Gargiulo, and D. Caputo*, "Enhanced visible-light-responsive photocatalytic property of CdS and PbS sensitized ZnO nanocomposite photocatalysts," *Materials Science and Engineering: B*, Vol. 177, No. 8, pp. 570-574, 2012.

[9] J. Bandara, U. Klehm, and J. Kiwi, "Raschig Rings-Fe_2O_3 composite photocatalyst activate in the degradation of 4-chlorophenol and orange II under daylight irradiation," *Applied Catalysis B: Environmental*, Vol. 76, No. 1-2, pp. 73-81, 2007.

[10] Y. Lu, L. Wang, D. Wang, T. Xie, L. Chen, and Y. Lin, "A comparative study on plate-like and flower-like ZnO nanocrystals surface photovoltage property and photocatalytic activity," *Materials Chemistry and Physics*, Vol. 129, No. 1-2, pp. 281-287, 2011.

[11] A. Yousef, N.A.M. Barakat, T. Amna, A.R. Unnithan, S. Al-Deyab, and H.Y. Kim, "Influence of CdO-doping on the photoluminescence properties of ZnO nanofibers: effective visible light photocatalyst for waste water treatment," *Journal of Luminescence*, Vol. 132, No. 7, pp. 1668-1677, 2012.

[12] X. Wang, G. Liu, G.Q. Lu, and H.M. Cheng, "Stable photocatalytic hydrogen evolution from water over ZnO–CdS core–shell nanorods," *International Journal of Hydrogen Energy*, Vol. 35, No. 15, pp. 8199-8205, 2010.

[13] R.K. Thareja, and A. Mohanta, "ZnO nanoparticles," In *Handbook of Nanophysics: Nanoparticles and Quantum Dots*, K.D. Sattler, ed.: CRC Press, Boca Ranton, Florida, United States, pp. 1-20, 2010.

[14] T. Olorunyolemi, A. Birnboim, Y. Carmel, O.C. Wilson Jr., and I.K. Lloyd, “Thermal conductivity of zinc oxide: from green to sintered state,” *Journal of the Ameriacan Ceramic Society*, Vol. 85, No. 5, pp. 1249-1253, 2002.

[15] M. Willander, O. Nur, Q.X. Zhao, L.L. Yang, M. Lorenz, B.Q. Cao, J. Zuniga Perez, C. Czekalla, G. Zimmermann, M. Grundmann, A. Bakin, A. Behrends, M. Al-Suleiman, A. El-Shaer, A. Che Mofor, B. Postels, A. Waag, N. Boukos, A. Travlos, H.S. Kwack, J. Guinard, and D. Le Di Dang, “Zinc oxide nanorod based photonic devices: recent progress in growth, light emitting diodes and lasers,” *Nanotechnology*, Vol. 20, No. 33, pp. 332001, 2009.

[16] R. Velmurugan, and M. Swaminathan, “An efficient nanostructured ZnO for dye sensitized degradation of reactive red 120 dye under solar light,” *Solar Energy Materials and Solar Cells*, Vol. 95, No. 3, pp. 942-950, 2011.

[17] Z. Shao, L. Wen, D. Wu, X. Zhang, S. Chang, and S. Qin, “AFM analysis of piezoelectric nanogenerator based on n^+-diamond/n-ZnO heterojunction,” *Applied Surface Science*, Vol. 257, No. 11, pp. 4919-4922, 2011.

[18] J. Livage, “Vanadium pentoxide gels,” *Chemistry of Materials*, Vol. 3, No. 4, pp. 578-593, 1991.

[19] Y. Wang, K. Takahashi, K.H. Lee, and G.Z. Cao, “Nanostructured vanadium oxide electrodes for enhanced lithium-ion intercalation,” *Advanced Functional Materials*, Vol. 16, No. 9, pp. 1133-1144, 2006.

[20] K. Zilberberg, S. Trost, H. Schmidt, and T. Riedl, “Solution processed vanadium pentoxide as charge extraction layer for organic solar cells,” *Advanced Energy Materials*, Vol. 1, No. 3, pp. 377-381, 2011.

[21] Y. Xu, and M.A. Schoonen, “The absolute energy positions of conduction and valence bands of selected semiconducting minerals,” *American Mineralogist*, Vol. 85, No. 3-4, pp. 543-556, 2000.

[22] M. Lee, and K. Yong, “Highly efficient visible light photocatalysis of novel CuS/ZnO heterostructure nanowire arrays,” *Nanotechnology*, Vol. 23, No. 19, pp. 1-6, 2012.

[23] S.Y. Pung, K.L. Choy, and X. Hou, “Structural and optical properties of ZnO nanostructures,” *ASEAN Engineering Journal Part B*, Vol. 1, No. 1, pp. 46-56 2012.